Title:

Persistent *Staphylococcus aureus* infections in children with chronic lung disease: a multi-omics analysis of bacterial adaptation to define novel therapeutic approaches

Short title: Persistent *S. aureus* infection in lungs

Xin Tan[1,2], Mathieu Coureuil[1,2], Elodie Ramond[1,2], Daniel Euphrasie[1,2], Marion Dupuis[1,2], Fabiola Tros[1,2], Julie Meyer[1,2], Ivan Nemanzny[1,4], Cerina Chhuon[1,3], Ida Chiara Guerrera[1,3], Agnes Ferroni[1,5], Isabelle Sermet-Gaudelus[1,6], Xavier Nassif[1,2], Alain Charbit[1,2*¶], Anne Jamet[1,2*¶]

[1] Université Paris Descartes; Sorbonne Paris Cité, Faculté de Médecine, Paris, France

[2] INSERM U1151 - CNRS UMR 8253, Institut Necker-Enfants Malades. Team: Pathogenesis of Systemic Infections, Paris, France

[3] Plateforme Protéome Institut Necker, PPN, Structure Fédérative de Recherche SFR Necker, University Paris Descartes, Paris, France

[4] Plateforme Métabolomique Institut Necker, Structure Fédérative de Recherche SFR Necker, University Paris Descartes, Paris, France

[5] Laboratoire de Microbiologie de l'hopital Necker, University Paris Descartes, Paris, France

[6] INSERM U1151 - CNRS UMR 8253, Institut Necker-Enfants Malades. Team: Canalopathies épithéliales : la mucoviscidose et autres maladies, Paris, France

¶AC and AJ are Joint Senior Authors

***Corresponding authors:** Alain Charbit, Anne Jamet.

e-mail: alain.charbit@inserm.fr (AC); anne.jamet@inserm.fr (AJ)

Abstract

Patients suffering from chronic lung diseases are abnormally colonized by many commensal and pathogenic bacterial species among which *Staphylococcus aureus* is the most commonly identified pathogen (prevalence in the lungs of cystic fibrosis (CF) patients greater than 70%). However, the mechanisms underlying the adaptation of *S. aureus* to the lung are poorly understood.

To get further insights into the molecular mechanisms of *S. aureus* adaptation to the chronic immunocompromised lung environment, we selected four pairs of sequential *S. aureus* isolates from 3 patients with CF and a patient with defective IgG antibody production suffering from chronic lung diseases. We used a combination of genomic, proteomic and metabolomic approaches with functional assays for in-depth characterization of *S. aureus* long-term persistence during chronic lung infection.

We demonstrate that chronic infection with *S. aureus* is related to the accumulation of genetic modifications inducing altered protein expression profiles and notable metabolic changes. These modifications are concordant with both patient-specific adaptation and convergent evolution of *S. aureus* isolates. We identified several metabolic pathways (*e.g.*, pantothenate and fatty acids) and virulence regulators (encoded by *agr* and *sae* loci) that could constitute therapeutic targets. Importantly, we show that long-term *S. aureus* infection leads to an increased ability to form biofilm and to a prolonged intracellular survival. Importantly, the increased ability to persist intracellularly was confirmed for *S. aureus* isolates within the own patient epithelial cells.

Our results strongly suggest that the intracellular environment might constitute an important niche of persistence and relapse necessitating adapted antibiotic treatments. Moreover, the multi-omics approach described in this study paves the way towards personalized medicine for the chronic infection management.

Author summary

Staphylococcus aureus is a well-known human pathogen causing both benign and life-threatening infections. Strinkingly, *S. aureus* has the ability to persist in the lungs of patients suffering from chronic respiratory disease for several years despite antibiotic therapies. Such a long-term persistence relies on a continuous within-host adaptation over time to cope with environmental pressures encountered in the lungs. In this study, we identified important genomic, proteomic and metabolic changes occurring during within-lungs adaptation of *S. aureus.* The pathways and virulence factors identified in this study as possibly leading to persistence may constitute novel therapeutic targets.

Introduction

The respiratory tract is a port of entry for external environment particles, such as microorganisms. In healthy individuals, infections are rare despite bacteria being inhaled frequently, due to sophisticated innate host defense mechanisms at the lung mucosa. Chronic bacterial infections are a hallmark of patients with cystic fibrosis (CF), chronic obstructive pulmonary disease (COPD) and primary immunodeficiency disorders with pulmonary manifestations [1-4]. These infections are associated with increased morbidity and contribute to a rapid decline in pulmonary function.

Staphylococcus aureus and *Pseudomonas aeruginosa* are the most common pathogens infecting the lungs of patients with a chronic lung disease [3, 4]. During chronic infections, pathogens have to adapt over time to cope with environmental pressures in the lungs such as inflammatory responses, hypoxia, nutrient deficiency, osmolarity modifications, low pH and antibiotic therapies [5-7]. The evolution of *P. aeruginosa* during chronic lung infections has been widely studied and includes acquisition of antibiotic resistances, increased exopolysaccharide production, loss in motility and formation of small colony variants (SCVs) [7-9]. In contrast, very few studies have addressed the adaptations undergone by *S. aureus* in patients with chronic lung diseases including CF [10, 11]. Moreover, each of these studies addressed only the genetic modifications occurring in isolates recovered from a single patient.

CF is one of the most frequent lethal autosomal recessive diseases among the Caucasian population. CF is caused by mutations in the cystic fibrosis transmembrane conductance regulator (CFTR) gene. CFTR dysfunction leads to thick sputum accumulation in the airways, explaining chronic bacterial infections and subsequent respiratory failure [2]. According to the CF patient registry of the US cystic fibrosis foundation, the prevalence of *S. aureus* among CF patients has increased from approximately 30% in 1990 to more than 70% in 2016 with peak prevalence between ages 11–17 years. Furthermore, *S. aureus* is one of the earliest bacteria detected in infants with CF.

Although mostly considered as a cause of acute infections with an extracellular lifestyle, *S. aureus* has the ability both to form biofilm [12-14] and to survive within a wide range of eukaryotic host cells [15-24]. These abilities likely contribute to the persistence of *S. aureus* in the airways of patients with chronic lung diseases for months or years despite appropriate antimicrobial treatments [25, 26].

S. aureus persistence is linked to a drastic decrease in metabolism (such as a reduction in the Krebs cycle activity) [27] and is generally associated with a decrease in the expression of virulence factors and an increase in the expression of bacterial adhesins [28]. Such profile is typical of small-colony variants (SCVs) that are defined by their slow growth rate resulting in small-sized colonies [22, 29, 30]. Beside SCVs, strains with normal colony morphology can exhibit similar patterns of "low toxicity" which allow them to persist intracellularly without being cleared by host cell defense mechanisms [28]. A "low toxicity" pattern can be achieved either transiently, by changes in the expression of genes encoding toxins and/or regulators, or permanently, by mutations in global regulators [31-33]. Indeed, during long-term infections, bacterial adaptation occurs through genomic modifications, including genome rearrangements and point mutations, that accumulate over time and lead to major modifications in protein expression [5]. These modifications result in the emergence of highly adapted clones that have the ability to better survive and persist in the airways of patients with chronic lung diseases than their ancestors.

To get further insights into the molecular mechanisms of *S. aureus* adaptation to the chronic immunocompromised lung environment, we selected four pairs of sequential *S. aureus* isolates from 3 patients with CF and a patient with defective IgG antibody production suffering from chronic lung diseases. We used a combination of next-generation sequencing and mass spectrometry approaches to detect proteogenomic variations, and integrated metabolomic and phenotypic approaches for in-depth characterization of *S. aureus* long-term persistence during chronic lung infection.

Altogether, the data presented reveal that persistence of *S. aureus* is associated with both patient specific adaptation and convergent evolution that explain increased ability to form biofilm as well as to survive within host cells. These observations should inform therapeutic decisions aiming at eradicating *S. aureus* chronic infections by choosing drugs targeting biofilm-embedded and intracellular bacteria.

Results

Selection of patients with *S. aureus* lung chronic infection.

The Necker-Enfants Malades Hospital (Paris, France) has collected clinical and microbiological information on patients with CF and other chronic lung diseases from 2008 onwards (hereafter named CP patients for chronically infected patients).

The CP1 patient (F508del +/+ CFTR mutation) was treated repeatedly with the association of rifampicine and fusidic acid for methicillin-resistant *S. aureus* (MRSA) and ciprofloxacine, ceftazidime and meropenem together with inhaled tobramycin or colimycin for *P. aeruginosa*. We selected an early isolate (CP1_early) from 2012 and a late isolate (CP1_late) from 2015.

The CP3 patient (F508del/R347P CFTR mutation) was treated with association of amoxicillin-clavulanate and trimethoprim-sulfamethoxazole (SXT) and also received occasionally minocycline and streptogramins during bronchial exacerbations. We selected an early isolate (CP3_early) from 2009 and a late isolate (CP3_late) from 2015.

The CP4 patient (F508del +/+ CFTR mutation) displayed a coinfection with *P. aeruginosa* requiring repeated intravenous antibiotics including ceftazidime, amikacin and ciprofloxacin. We selected an early isolate (CP4_early) from 2008 and a late isolate (CP4_late) from 2017.

The CP2 patient was not CFTR mutated but exhibited a primary humoral immunodeficiency disorder with a mild IgG2 deficiency causing chronic bronchitis. Bronchial exacerbations were treated with SXT association. We selected an early isolate (CP4_early) from 2009 and a late isolate (CP4_late) from 2013.

Clonal relationship between *S. aureus* sequential isolates.

The clonal relationship of serial CP isolates was investigated with whole-genome sequencing and *in silico* multilocus sequence typing (MLST). We confirmed that each pair of isolates of each single patient had the same unique sequence type and, hence, belonged to the same clone.

The four pairs of isolates belonged to four distinct clones (ST8 for CP1 patient, ST15 for CP3 patient, ST5 for CP4 patient and a double loci variant of ST45 for CP2 patient), separated by 3 to 9 years intervals. We used four publically available reference strains and generated a dendrogram showing clusterisation of isolates of each patient with the chosen reference strain (see Methods) (**Fig 1**).

Genomic analysis of *S. aureus* adaptation during long-term infection of lungs.

Genomes of all clinical isolates were *de novo* assembled and coding DNA sequences (CDSs) were annotated. Basic assembly metrics are available in **S1 Table**. Predicted proteins were further classified in functional eggNOG categories. Genomic evolution was studied by single-nucleotide

polymorphisms (SNPs), short insertions and deletions (indels) analysis and the search of larger deletion/insertion events. General features of detected mutations are showed in **Table 1**. As expected, the total number of polymorphisms increased with the amount of time separating the early and late isolates. Most of the SNPs were missense variants occurring in CDSs. As frequently observed during long-term within-host evolution of clones [11, 34, 35], a genome reduction was evidenced for the 4 clones with late isolates having reduced genome size (with a genetic loss ranging from 10 to 81 kb) compared to early isolates (**S1 Table**). Large deletions were plasmids or prophage regions lost during chronic infection (**S2 Table**).

Of note, nonsynonymous mutations acquired by late isolates were found mainly in genes involved in metabolic processes (**Fig 2A**) and more specifically in “amino acid transport and metabolism” and “carbohydrate transport and metabolism” functional categories (**S3 Table**) (*e.g.*, *trpA* and *serA* genes). Nonsynonymous mutations acquired by late isolates were also frequently found in the “information storage and processing” category which encompasses proteins involved in replication, translation and repair processes (*e.g.*, *polC* and *holB* genes). Genetic variations in virulence genes encompass missense mutations in genes encoding highly variable surface proteins such as the protein A and SdrH. The protein A alteration could result in the reduction of *S. aureus* ability to trigger inflammation [36].

We assumed that the early *S. aureus* isolates were already present in lungs of the CF patients for several months or years at the time of sampling and, thus, probably had already acquired adaptive mutations. Therefore, we first searched for nonsynonymous mutations in these early isolates compared to reference strains. We focused on mutations likely to have the greatest impact (*i.e.*, premature stop codon) and found that **CP1_early** had premature stop codons in *hisD, rarD* and *ausA* genes; **CP2_early** in *sdrC*; **CP3_early** in *trpE;* and **CP4_early** in *secA1* (**S4 Table)**. During chronic infections, convergent evolution most likely occurs in response to a common selection pressure, the most common one being antibiotic treatment. Therefore, we searched in our sequenced genomes, loci that were independently altered by nonsynonymous mutations in multiple isolates, which could be an indication of adaptative parallel evolution. Remarkably, we found that 12 genes had nonsynonymous mutations in *S. aureus* isolates from at least three out of the four CP patients (SAUSA300_0203, *mtlR, sdrC, ebh, tagB, cvfC, gatA, agrC, lctP2, clpL, feoB, asp2*) when compared to reference strains (**S5 Table)**.

We next searched for nonsynonymous mutations in the late isolates compared to cognate early isolates and found four genes mutated in the late isolate of at least two patients (**S4 Table**). These four genes encode: i) SaeR, a regulator involved in the control of exoproteins expression, ii) the FakA fatty acid kinase A, involved in biofilm formation [13] and virulence genes expression [37], iii) the ThyA thymidylate synthase, involved in pyrimidine metabolism whose inactivation confers SCV phenotype and SXT resistance, and iv) the very large cell-wall associated fibronectin-binding protein Ebh.

Table 1. General features of detected mutations

	CP1_late	CP2_late	CP3_late	CP4_late
Time since early isolate	2.8 years	4.4 years	6.7 years	9 years
Total polymorphisms	21	30	34	79
SNP[a]	19	26	25	73
INDEL[b]	2	4	9	6
CDS[c]	18	23	21	62
NON-SYN[d] (%)	14 (77.8)	17 (56.7)	16 (47.1)	51 (64.6)
FR[e]	2	2	4	4
MS[f]	10	14	11	47
STOP gained[g]	1	1	1	0
Other	1	0	0	0
SYN[h]	4	6	5	11
IG[i]	3	7	13	17

[a]SNP, single nucleotide polymorphism; [b]INDEL, insertion-deletion; [c]CDS, coding sequence; [d]NON-SYN, nonsynonymous mutation; [e]FR, frameshift variant; [f]MS, missense variant; [g]STOP gained, premature stop codon; [h]SYN, synonymous mutation; [i]IG, intergenic

Whole cell proteomic analyses of early and late *S. aureus* isolates.

The four pairs of isolates were harvested for proteomic analysis at post exponential growth phase. Differences in the expression of proteins of each late isolate were analyzed and compared to their

cognate early isolate **(Fig 3A, Fig S1A)**. We focused on proteins with a detection difference of at least 2 in log2(intensity) after normalization.

Total proteins were extracted, digested into peptides and analyzed by LC-MS/MS mass spectrometry. Detected peptides were mapped against a custom database containing USA300 (NC_007793.1) proteins and all predicted proteins from genome annotation of clinical isolates.

Functional categories of proteins. Proteins were classified within eggNOG functional categories. The largest category of proteins to be differentially expressed for all pairs comprised proteins related to metabolism processes (and more specifically to the "amino acid transport and metabolism" category) (**Fig 2A**; **S7 Table**). Notably, for three patients, the expression of proteins involved in the urea degradation and/or arginine biosynthesis pathways was modified in late isolates compared to early isolates.

Altogether, the functional category "amino acid transport and metabolism" appeared to be the most affected both in terms of genetic modifications and of levels of protein expression, suggesting the central role of the corresponding pathways during within-host adaptation.

The category "cellular processes and signaling", encompassing regulatory proteins, was second largest category of proteins to be differentially expressed. Indeed, proteins of the Agr, Rot, Sae, Sar or Fur regulatory networks were differently expressed in all late isolates. Besides, SdrD, which plays a role in adhesion, invasion, and immune evasion [38], was up-regulated in late isolates of three patients. In addition, the protein SAUSA300_1236 (annotated as a CAP domain-containing protein of unknown function) was down-regulated in late isolates of three patients.

Protein profiles. In CP1 patient, the *agrC* gene mutation found in the late isolate had a pleiotropic effect on the proteome. Indeed, delta hemolysin, PSMb1 and AgrA were down-regulated in the late isolate whereas proteins encoded by *spa, sbi, fnbA, rot* and *coa* genes were up-regulated. In addition, adhesins encoded by *sasG, efb, sdrD* and *ecb* were up-regulated. Altogether, this expression pattern suggests that the CP1 late isolate has evolved low virulent and highly adhesive properties.

In CP2 patient, a mutation in the *thyA* gene was found in the CP2_late isolate. Strikingly, products of operon *pabBC* (involved in folate biosynthetic pathway) were up-regulated likely to compensate the thymidylate synthase dysfunction [39]. In contrast to what is typically described in *thyA* mutants [40], AgrA and AgrC were up-regulated in CP2_late isolate, leading to the concomitant up-regulation of *hld*

and *geh* genes products and to FnbA down-regulation. This expression pattern suggests that the CP2 late isolate have retained virulent properties.

In CP3 patient, the *thyA* gene mutation found in the late isolate was coupled to a down-regulation of the *agr* regulon (leading to the down-regulation of *hld*, *saeP*, *lip* and *geh* gene products) [40]. This expression pattern suggests that, as for the CP1 late isolate, the CP3 late isolate has evolved toward low virulent and highly adhesive properties. In addition and as expected, products of *dinG* and *thiM* genes, which harbored a frameshift, and *thyA*, which harbored a premature stop codon, were not detected in CP3_late isolate compared to CP3_early isolate.

In CP4 patient, frameshifts in *fakA* and *panB* genes were associated with a lack of cognate proteins expression in CP4_late isolate. Of note, a defect in *fakA* expression has been associated with an increased biofilm formation ability [13] and a downregulation of the SaeR regulon [37]. Besides, a defect in *panB* expression has been previously associated with pantothenate auxotrophy and persistence [41]. We confirmed both pantothenate auxotrophy (**Fig 4**) and an increased biofilm formation in CP4_late isolate (**Fig 5**) (see below). In addition, adhesins encoded by *sdrD* and *sasF* were upregulated suggesting a hyper adhesive phenotype.

Altogether, the proteogenomic data suggest that all the late isolates, but CP2_late, have evolved toward highly adhesive and low virulent properties.

Whole cell metabolomic analyses of early and late *S. aureus* isolates.

In parallel with the proteomic analyses described above, the four pairs of isolates were harvested for targeted metabolomic analysis at post exponential growth phase. This analysis, performed using mass spectrometry, allowed us to measure relative concentrations of central and intermediary metabolites from a number of metabolic pathways including glycolysis/gluconeogenesis, pentose-phosphate pathway, TCA cycle, nucleotides biosynthesis, free fatty acids, coenzymes and amino acids.

Functional categories of metabolites. Detected metabolites were classified in 8 categories (**Fig 2B**). Strikingly, the most altered category in the late isolate of all four patients, compared to their cognate early isolates, was the amino acid category. These findings are concordant with proteogenomic results and confirm the central role of amino acid metabolism during within-host adaptation.

Metabolite profiles comparisons. The difference in metabolic profiles between early and late isolates of CP patients is highlighted by heatmaps shown in **Fig S1B** and **Fig 3B**. A list of metabolites with altered amount in the four pairs of isolates is provided in **S8 Table**.

In CP1 patient, the metabolite profiling, which shows a marked reduction of citrate and cis-aconitate, clearly indicates a reduced citric acid cycle activity. A drastic decrease in arginino-succinate is observed and is in line with an increase of ArgF, ArgG and ArgH proteins found in proteomic analysis.

In CP2 patient, a drastic decrease in ornithine is probably caused by a diminution of ArcA protein (arginine deiminase) found in proteomic analysis. Indeed, arginine fermentation into ornithine relies on the *arc* operon. A severe reduction of threonine amounts was also recorded. In *S. aureus*, threonine is synthesized from aspartate and serves itself as a precursor for the synthesis of the branched-chain amino acid isoleucine. Of note, the threonine biosynthetic pathway has been shown to be essential for *S. aureus* virulence in mice and is important for staphylococcal bloodstream infection [42].

In CP3 patient, a decrease in phosphoenolpyruvate is correlated with a diminution of GapB (glyceraldehyde 3-phosphate dehydrogenase) protein, whereas a decrease in ADP is correlated with the lack of ThiM (hydroxyethylthiazole kinase) expression found in proteomic analysis (due to a frameshift in *thiM* gene).

In CP4 patient, a drastic diminution of pantothenate, coenzyme A and dephospho-coenzyme A is in line with the frameshift in *panB* gene and the subsequent lack of expression of PanB and PanC proteins. Indeed, the pantothenic acid is a precursor of coenzyme A [43]. In addition, cystine and cystathionine were dramatically decreased. In bacteria, cysteine is synthesized from serine by incorporation of sulfide or thiosulfate. Cysteine-containing molecules such as glutathione and thioredoxin play a major role in maintaining an intracellular reducing environment and protection against oxidative stress. In *S. aureus*, free cysteine, reduced coenzyme A, and other thiols may help maintain the thiol redox balance. Hence, a defect in cysteine biosynthesis is likely to affect protein synthesis and *S. aureus* starvation survival. Besides, as for CP3 patient, a decrease in phosphoenolpyruvate is correlated with a diminution of GapB protein and as for CP1 patient, there is a reduced citric acid cycle activity with a marked reduction of citrate and cis-aconitate.

Moreover, in CP2_late and CP3_late isolates that display a *thyA* gene alteration (associated with a SCV phenotype, see below), we found a decrease in asparagine, which is consistent with previous findings showing a decrease in aspartate in SCVs [27]. Asparagine is directly link to the citric acid

cycle through the oxaloacetate intermediate; hence a decrease in asparagine is associated with a reduced citric acid cycle activity.

Altogether, metabolic profiling suggests that the four late isolates have evolved a reduced citric acid cycle activity compared to cognate early isolates.

Functional characterization of the *S. aureus* isolates.

We first examined growth of the four pairs of isolates in broth (on solid media and in liquid culture; **Fig 4, Fig S2 and Fig S3**), determined their antibiotic susceptibility profiles and their capacity to form biofilm (**Fig S4 and Fig S5**).

Growth properties in broth. Colony morphology on brain heart infusion (BHI) agar plates was similar to that of USA300-LAC or slightly smaller for all isolates, except for late isolates of CP2 and CP3 patients that displayed a typical SCV phenotype with very small colonies (**Fig S2**). CP2_late and CP3_late isolates also failed to grow on Mueller-Hinton plates, suggesting that they had acquired an auxotrophy for at least one of the compounds absent in the Mueller–Hinton agar medium, such as thymidine, hemin, or menadione (that are present in BHI). Since thymidine-dependent SCVs have been shown previously to be frequently isolated from the airways of CF patients [44], we first monitored growth of the two SCV-like isolates in a defined medium mimicking the respiratory fluid of cystic fibrosis patients (Cystic Fibrosis Sputum Medium or CFSM) [45] (**Fig 4**). As anticipated, CP2_late and CP3_late isolates exhibited a severe growth defect in the absence of thymidine whereas supplementation with thymidine restored almost wild-type growth (*i.e.,* similar to that recorded with USA300-LAC, **Fig 4B**). As previously mentioned and in line with these observations, genomic analysis identified a mutation in the *thyA* gene for both isolates. Besides, CP4_late isolate displayed a moderate reduced growth compared to USA300-LAC that was not corrected by adding thymidine in the medium (not shown). As previously mentioned, genomic analysis of CP4_late isolate showed a frameshit in *panB* gene, which is involved in *de novo* biosynthesis of pantothenic acid. Indeed, growth of CP4_late isolate in the presence of pantothenate restored wild-type growth (**Fig 4C**).

Antibiotic susceptibility. Antibiotic susceptibility assays showed that isolates of CP1 and CP4 patients were resistant to methicillin, whereas isolates of CP2 and CP3 patients were methicillin susceptible. Besides, the 2 SCV isolates (CP2_late and CP3_late) were resistant to SXT, which is consistent with the fact that both patients received this antibiotic. A P48R mutation and a premature

stop codon (W88X) were detected in *thyA* gene in CP2_late and CP3_late genomes, respectively, fully supporting the thymidine auxotrophy and SXT resistance of these isolates.

Of note, the late isolate of CP4 patient acquired a resistance to fluoroquinolones, consistent with the administration of ciprofloxacin to this patient. A F226S mutation, detected in *gyrB* gene in CP4_late genome, could account for this fluoroquinolones resistance. The late isolate of CP3 patient acquired a resistance to cyclines consistent with the administration of minocycline in this patient. A K57M amino acid substitution in the ribosomal S10 gene was detected in CP3_late genome. Remarkably, two clinical *S. aureus* isolates with mutation in this same region of the S10 protein (a deletion of residues 56 to 59; and double mutant K57M, Y58F) have been recently shown to confer resistance to tigecyclin [46].

Biofilm formation. Bacteria often grow in organized communities known as biofilms, which favor their persistence. Assuming that isolates retrieved from chronic infections might have a higher biofilm-forming capacity than isolates retrieved from acute infections, we studied biofilm-forming capacities of the four pairs of isolates. Remarkably, the eight clinical isolates displayed a greater capacity to form biofilms, compared to USA300-LAC reference strain (p-value of <0.001, **Fig S4**). Furthermore, for three patients, the late isolates formed more biofilm than the early isolates, suggesting that long-term adaptation had improved their biofilm formation capacity (p-value of <0.001, **Fig S5**).

S. aureus isolates exhibit an increased persistence within CFBE-F508del epithelial cell line.

Numerous studies have shown that intracellular survival is likely to play an important role in long-term infection [16]. Moreover, our results evidenced that most alterations found in coding sequences, protein expression and metabolites impact metabolic pathways and especially amino-acids metabolism, which suggests nutritional adaptation to a niche. We therefore thought to test if this nutritional adaptation could favor intracellular persistence.

To evaluate the capacity of *S. aureus* isolates to persist intracellularly, we infected both bronchial CFBE epithelial cell line 41o- (homozygous for the F508del-CFTR mutation) and CFBE with a plasmid allowing wild type CFTR expression. We tested the 4 pairs of clinical isolates, the control strain USA300-LAC and a stable SCV mutant altered in the haemin biosynthetic pathway (hereafter named

339 Δ*hem*). The infection was pursued for 6 days, using gentamicin protection assay to prevent
340 extracellular bacterial growth, as previously described [20]. As expected, the number of wild-type
341 intracellular bacteria dramatically decreased during the course of infection whereas the Δ*hem* mutant
342 was able to persist intracellularly during the whole course of the experiment (**Fig S5**). Strikingly, at day
343 6 post-infection, all clinical isolates were able to persist at least 19-fold and up to 452-fold more than
344 the USA300-LAC reference strain (**Fig 6**). For the 3 patients with cystic fibrosis, the late isolates
345 exhibited an improved ability to persist intracellularly within CFBE-F508del epithelial cells compared to
346 cognate early isolates at day 6 post-infection (**Fig 6**). Of note, this was not observed for CP2, which is
347 not a CF patient. Interestingly, the two late isolates with thymidine auxotrophy (*i.e.*, CP2 and CP3 late
348 isolates) had a reduced ability to persist within CFBE expressing wild type CFTR (CFBE-WT) epithelial
349 cells, whereas at day 6 post-infection, those thymidine auxotroph isolates persist better or equally well
350 than cognate early isolates within CFBE-F508del epithelial cells (**Fig 6, Fig S6**).
351

352 **Late *S. aureus* isolate of CP4 patient exhibits an increased persistence within**
353 **primary F508del epithelial own patient cells.**

354 The CP4 patient exhibits a F508del +/+ CFTR mutation. To confirm the relevance of the results
355 obtained with bronchial CFBE epithelial cell line, we assessed the persistency of CP4 isolates within
356 primary epithelial cells isolated from the nose of the CP4 patient and from a healthy donor. This
357 experiment provides a unique opportunity to verify the specific within patient-adaptation of *S. aureus*
358 recovered from long-term infection. The experiment (performed once in triplicate) confirmed that the
359 late isolate persistence ability is improved compared to early isolate at day 3 and 6 within both primary
360 nasal epithelial cells retrieved from a healthy donor and from the CP4 patient **(Fig 7)**.
361
362

363 # Methods

364 ## Patients and bacterial isolates

365 Nasal epithelial cell (HNE cells) were sampled by nasal brushing of both nostrils after local
366 visualization of the nasal mucosa from one healthy volunteer and patient CP4.

The epidemic clone *S. aureus* USA300-LAC (designated WT) was provided by the Biodefense and Emerging Infections Research Resources (BEI). A derivative of USA300-LAC with a deletion in the haemin pathway (*ΔhemDBL* triple deletion mutant), involved in the electron transport system, has been previously constructed to obtain a strain with a stable SCV-phenotype [20].

S. aureus isolates were grown on brain heart infusion (BHI) broth and agar plates. Colony morphotypes were assessed after 24h of growth on BHI or Mueller-Hinton agar plates.

When indicated, *S. aureus* isolates were cultured in medium mimicking the respiratory fluid of cystic fibrosis patients (Cystic Fibrosis Sputum Medium or CFSM) [45] with or without the addition of thymidine (100 µg/mL) or pantothenate (50 µg/mL).

Whole-genome sequencing and analysis

Genomic DNA was extracted using DNeasy Blood and Tissue Kit with 10 µg/mL lysostaphin to facilitate cell lysis. Genomic libraries were prepared using a Nextera XT kit, multiplexed and sequenced on an Illumina MiSeq instrument (2x150 paired-end sequencing).

The short reads were processed using the Nullarbor bioinformatic pipeline software v1.20 (Available from: https://github.com/tseemann/nullarbor). Briefly, raw reads were trimmed using trimmomatic [47], de novo assembled using SPAdes 3.9.0 [48] and annotated using Prokka v1.11 [49]. Single nucleotide polymorphisms (SNPs) and small indels were assessed using Snippy v3.1 (https://github.com/tseemann/snippy). The Similar Genome Finder Service of the PATRIC 3.5.2 on-line database was used to identify the most similar publically available genome for each pair of clinical isolates (https://www.patricbrc.org/app/GenomeDistance). Snippy was used both to map reads of late isolates against the annotated assembly of the early isolate and to map reads of early and late isolates against the publically available closest reference genome for the four pairs. Snippy classifies variants by their predicted functional effect based on mapping to the annotated reference genome in synonymous, nonsynonymous or truncating for protein-coding sequences.

Assemblies generated by Nullarbor were uploaded in RAST server [50] and were also annotated through the RAST annotation pipeline with ClassicRAST annotation scheme. The ‘Sequence Based Comparison Tool’ of the RAST server, which is based on BLAST protein similarity search, was used to identify large insertions and deletions of each late isolate compared to early isolate as a reference.

The sequences reported in this paper are available at NCBI’s BioProject database under accession number PRJNA446073 (http://www.ncbi.nlm.nih.gov/bioproject/446073).

Quantification of biofilm formation

To determine biofilm formation in static conditions, clinical isolates as well as reference strains were cultured in Brain Heart Infusion (BHI) medium in the presence of 1% glucose. The reference strains include USA300-LAC that is a weak biofilm producer and its *ΔagrC* derivative that is a strong biofilm producer (obtained from the BEI Nebraska Transposon Mutant Library). The over-night cultures were diluted to an OD600nm of 0.05 in fresh BHI medium supplemented with 1% glucose. A total of 200 µl of each diluted culture were inoculated in two polystyrene 96-well plates in triplicate and incubated for 48 hours at 37 ° C without shaking. After 24 h of growth, the medium was renewed. After 48 h, one of the 96-well plates was used to assess bacterial growth by taking into account both bacteria in suspension and adherent bacteria (resuspended mechanically) and measuring OD600nm. The other 96-well plate was used to quantify biofilm formation. The wells were washed three times with distilled H_2O to remove unattached bacteria and the biofilm fixed at the bottom of the wells was stained with 100 µl 2 % crystal violet solution for 15 min. After staining, wells were washed three times with distilled H_2O. Crystal violet was solubilized using 150 µl of acetic acid at 30 %. 100 µl of the solubilized dye was transferred to a new 96-well plate to determine the absorbance at 540 nm.

Antimicrobial susceptibility

Antimicrobial susceptibility of isolates was evaluated by disc diffusion method. Etests were used to determine minimal inhibitory concentrations to gentamicin. Susceptibility tests were carried out on BHI agar plates to allow the growth of auxotrophic isolates.

Cell culture experiments

Cystic Fibrosis Bronchial Epithelial cell line CFBE41o- that is an immortalized cell line homozygous for the delF508 mutation and the CFBE cell line complemented to express WT CFTR were generously provided by Dieter Gruenert (University of California, San Francisco) [51]. They were cultured in Minimum Essential Medium (MEM) supplemented with 10% fetal bovine serum (FBS) and containing 300µg/mL hygromycin B, 1% penicillin/streptomycin and 1% amphotericin B.

Primary nasal epithelial cell (HNE) were obtained as described in [52] and cultured in Dulbecco's Modified Eagle's medium mixed 1:1 with Ham's F-12 (DMEM:F12) supplemented with 10% FBS, 1%v/v non-essential amino acids, 90 µg/10 µg/ml Piperacillin/Tazobactam and 1% amphotericin B.

Prior infection assays, epithelial cells were seeded in uncoated wells for CFBE and wells coated with collagen for HNE and all antibiotics were removed from culture medium. Epithelial cells were

infected with a multiplicity of infection (MOI) of 100 using an inoculum taken from cultures of *S. aureus* grown in BHI until exponential growth phase. After 1h30, each well was washed three times with 1 mL of phosphate buffer saline (PBS) containing 300 µg/mL gentamicin, to remove extracellular bacteria. Washing and addition of fresh medium containing 50 µg/mL gentamycin were repeated at day 3. Gentamicin has a high bactericidal effect on *S. aureus* USA300 (minimum inhibitory concentrations (MIC) = 2 $\mu g.mL^{-1}$) and a very poor penetration inside eukaryotic cells. In addition, the measured MIC of gentamicin of all clinical strains was below or equal to 2 $\mu g.mL^{-1}$. Infected cells were kept in a humidified 5% CO2 atmosphere at 37°C for 6 days. To enumerate viable intracellular persisting bacteria, the culture medium containing gentamicin was removed from infected cells and wells were washed three times with antibiotic free PBS. Epithelial cells were lysed by scrapping with 1mL of distilled water during 15 minutes and serial dilutions of the cell lysates were plated on BHI agar. Colony forming units were numerated after 48 h at 37°C. Results shown are normalized with USA300-LAC strain as a reference and expressed as a fold change of CFUs.

Proteomic analyses

S. aureus isolates were grown in CFSM with addition of thymidine (100 µg/mL) in technical triplicate and collected after 19h of growth at 37°C with agitation (*i.e.*, at post exponential growth phase). Bacteria were lysed in PBS containing CaCl2 1 mM, MgCl2 1 mM and 10µg/mL lysostaphin.

Proteins were digested and analyzed by liquid chromatography coupled with tandem mass spectrometry (nanoLC-MS/MS). Filter Aided Sample Preparation (FASP) was used for protein digestion [53, 54]. Proteins were then reduced in 100 mM DTT for 30 min at 60°C, mixed with 8 M urea buffer, loaded on Microcon 30kDa centrifugal filters (Millipore) and alkylated with 50 mM iodoacetamide. Filters were washed twice with 8 M urea and twice with 50 mM ammonium bicarbonate. Following an overnight trypsin digestion at 37°C, samples were vacuum dried, and kept at −20 °C until MS analysis.

MS analysis was performed as previously published [54]. Dried peptides were resuspended in 10% ACN, 0.1% TFA. For each run, 5 µl (corresponding approximately to 1 µg of peptides) were injected in a nanoRSLC-Q Exactive PLUS MS (Dionex RSLC Ultimate 3000, Thermo Scientific, Waltham, MA). Peptides were separated on a 50 cm reversed-phase liquid chromatographic column (Pepmap C18, Dionex). Chromatography solvents were: (A) 0.1% formic acid in water, and (B) 80% acetonitrile with 0.08% formic acid. Peptides were eluted from the column with the following gradient: 5% to 40% of B

for 120 min and then 40% to 80% of B in 1 min. At 125 min, the gradient was reversed to 5% to allow re-equilibration of the column for 20 min before the next injection. One blank with two 30 minutes linear gradients was run between triplicates to prevent sample carryover.

Peptides eluted from the column were analyzed by data dependent MS/MS, using the top-10 acquisition method. Briefly, the instrument settings were as follows: resolution was set to 70,000 for MS scans and 17,500 for the data dependent MS/MS scans in order to increase speed. The MS AGC target was set to 3.10^6 counts, whereas the MS/MS AGC target was set to 5.10^4. The MS scan range was from 400 to 2000 m/z. MS and MS/MS scans were recorded in profile mode. Dynamic exclusion was set to 20 s duration. Each sample was analyzed in three technical triplicates by nanoLC/MS/MS. Raw MS files were processed with the MaxQuant software version 1.5.8.3 and searched with the Andromeda search engine against a custom protein database containing 3 457 protein sequences. To build this database we pooled protein sequences from both PROKKA and RAST annotations of all clinical isolates and the MAGE annotation of USA300 (NC_007793.1) [55]. Redundancy of the sequence set was reduced using CD-HIT v4.6 [56] with a 80% identity threshold. To search for parent mass and fragment ions, we set the mass deviation at 4.5 ppm and 20 ppm, respectively. The minimum peptide length was set to seven amino acids and strict specificity for trypsin cleavage was required, allowing up to two missed cleavage sites. Match between runs was allowed. Carbamidomethylation (Cys) was set as fixed modification, whereas oxidation (Met) and protein N-terminal acetylation were set as variable modifications. The false discovery rates (FDRs) at the protein and peptide level were set to 1%. Scores were calculated in MaxQuant as described previously [57]. The reverse and common contaminants hits were removed from MaxQuant output. Proteins were quantified according to the MaxQuant label-free algorithm using normalized label free quantification (LFQ) intensities. Protein quantification was obtained using at least two peptides per protein.

Statistical and bioinformatic analysis, including heatmaps and clustering, were performed with Perseus software (version 1.6.0.7) freely available at www.perseus-framework.org [58]. EggNOG annotations of all proteins were retrieved from webserver (last accessed 2017-12-15) [59]. Gene names were retrieved from AureoWiki [60] (last accessed 2017-12-15). Extraction of annotations GO, Keywords, EggNOG and Kegg pathway were performed using Perseus.

For accurate quantification, we analysed each isolate separately (3 samples from early and 3 samples from late collection). We filtered the data to keep only proteins with at least 3 valid values in

at least one group (late or early). Next, the data were imputed to fill missing data points by creating a Gaussian distribution of random numbers with a standard deviation of 33% relative to the standard deviation of the measured values and a 2.5 standard deviation downshift of the mean to simulate the distribution of low signal values. To discriminate differential protein amongst early and late for each isolate we performed an t-test, S0=0.1, and retained only proteins with an FDR<0.05. Hierarchical clustering of significantly different proteins was performed in Perseus on logarithmic LFQ intensities after z-score normalization of the data, using Euclidean distances and default parameters. We also performed a T Test, S0=0.1, FDR=0.001 to discriminate differential proteins between late and early.

Metabolomic analyses

Metabolite profiling of *S. aureus* isolates was performed by liquid chromatography–mass spectrometry (LC-MS) as described [61]. Briefly, *S. aureus* isolates were grown in CFSM with addition of thymidine in the same conditions as for the proteomic analyses. Metabolic activity was blocked by immersion in liquid nitrogen for 10 sec. Metabolites were extracted using a solvent mixture of Methanol/ACN/H2O (50:30:20) at −20 °C. Samples were vortexed for 5 min at 4°C, and then centrifuged at 16,000 g for 15 minutes at 4°C. The supernatants were collected and analysed by LC-MS using SeQuant ZIC-pHilic column (Millipore) for the liquid chromatography separation [61]. The aqueous mobile-phase solvent was 20 mM ammonium carbonate plus 0.1% ammonium hydroxide solution and the organic mobile phase was acetonitrile. The metabolites were separated over a linear gradient from 80% organic to 80% aqueous phase for 15 min. The column temperature was 48 °C and the flow rate was 200 µl/min. The metabolites were detected across a mass range of 75–1,000 m/z using the Q-Exactive Plus mass spectrometer (Thermo) at a resolution of 35,000 (at 200 m/z) with electrospray ionization and polarity switching mode. Lock masses were used to insure mass accuracy below 5 ppm. The peak areas of different metabolites were determined using TraceFinder software (Thermo) using the exact mass of the singly charged ion and known retention time on the HPLC column. By this approach we were able to identify and measure: Glucose, Glucose-6P (G6P), UDP-glucose (UDP-Glc), Sedoheptulose-7-P (SH-7P), Ribose 5-phosphate, Glyceraldehyde 3-phosphate, Lactate, Pyruvate, Phospho-Enol-Pyruvate (PEP), Citrate (Cit), cis-aconitate (cis-aco), Succinate (Suc), Fumarate (Fum), Malate (Mal), alpha ketoglutarate (aKG), dihydroxyacetone phosphate (DHAP), N-carbamoyl-L-aspartate, Nicotinamide adenine dinucleotide (NAD), NADH, Nicotinamide adenine dinucleotide phosphate (NADP), NADPH, Adenine, Adenosine, Adenosine Mono, Di and Tri-

phosphate (AMP, ADP, ATP), Cytidine, Cytidine Mono, Di and Tri-phosphate (CMP, CDP, CTP), Uridine Mono, Di and Tri-phosphate (UMP, UDP, UTP), Hypoxanthine, Guanine, Guanaosine, Guanidine Mono and Di-phosphate (GMP, GDP), Inosine monophosphate (IMP), Pantothenate, Dephospho-Coenzyme A, Coenzyme A (CoA), Flavin adenine dinucleotide (FAD), Niacin, Nicotinamide, 3-hydroxybutyrate, Urate, 5-oxo-L-Proline, Acetyl-aspartate, Acetyl-glutamine, Alanine, Arginine, Argininosuccinate, Asparagine, Aspartate, Betaine, Citrulline, Cystathionine, Cystine, Glutamine, Glutamate, Glycine, Histidine, IsoLeucine, Leicine, Sarcosine, Lysine, Methionine, Ornithine, Phenylalanine, Proline, Serine, Taurine, S-Adenosyl-L-methionine, Threonine, Tryptophan, Tyrosine, Valine, Butyric acid, Carnitine, Decanoic acid, Lauric acid, Hexanoic acid, Linoleic acid, Myristic acid, Octanoic acid, Oleic acid, Palmitic acid.

Statistical analyses were performed using MetaboAnalyst 4.0 software [62]. The algorithm for heatmap clustering was based on the Pearson distance measure for similarity and the Ward linkage method for biotype clustering. Metabolites with similar abundance patterns were positioned closer together.

Statistical analysis

Data were analyzed using Excel or GraphPad Prism softwares. Results are presented either with one representative experiment or as means ± standard deviation (SD). The number of biological and technical replicates is indicated per figure.

For two-sample comparisons statistical significance was measured using unpaired two-tail Student's t-test. For comparisons between more than two groups, statistical significance was measured using one-way analysis of variance (ANOVA) with multiple comparisons (Dunnett's correction) performed, with each value compared to that of the reference strain.

P values of <0.05 were considered to indicate statistical significance.

Ethics statement

All experiments were performed in accordance with the guidelines and regulations described by the Declaration of Helsinki and the low Huriet-Serusclat on human research ethics and informed consent was obtained for all participating subjects. Serial isolates of *S. aureus* were obtained from airway secretions from four patients with chronic lung infection at the Necker-Enfants Malades University Hospital, Paris, France. Sputum sampling is part of routine standard care. The research procedure is validated by Ile de France 2 IRB (ID-RCB/Eudract: 2016 A00309-42).

Discussion

Our study revealed patient-specific adaptation, illustrated by the acquisition of mutations leading to antibiotic resistances directly correlated to the drugs administered to the patient. Our study also provided evidence for the acquisition of common adaptive traits, such as SCV phenotype, antibiotic resistances, auxotrophies, reduced citric acid cycle activity, increased biofilm and intracellular persistence abilities that occurred irrespective of the clone type.

Of particular interest, we report mutations in two master regulatory systems, Agr and Sae, likely to impact multiple proteins expression and metabolites amounts.

agr-defective mutants have been shown to arise during chronic infections and are better adapted to persistence within the infected host [32, 63, 64]. The CP1 late isolate is typical of *agr*-defective mutants with up-regulation of adhesins and downregulation of toxins evidenced by proteomic analysis.

Genetic alterations directly or indirectly targeting SaeR regulon were identified in the 3 CF patients. Since SaeR is involved in the regulation of over 20 virulence factor genes [65] and SaeRS-deficient bacteria are less infective in animal models [66], it is likely that long-term colonization is associated to reduced virulence.

In CP1, CP3 and CP4 late isolates, we observed an increased in the expression of the SdrD adhesin belonging to the SaeR regulon [67] (**S7 Table**), suggesting that SdrD is also important for long-term lung colonization. Of note, SdrD is involved in adhesion to human nasal epithelial cells and to human keratinocytes [68].

In patients with chronic lung infections, SCVs detection is most often the consequence of a long-term SXT treatment [69]. These stable clinical SCVs isolates are no longer susceptible to SXT and are thymidine-auxotrophic (TA-SCV) due to mutations in the *thyA* gene encoding the thymidylate synthase [44, 69]. Remarkably, *thyA* mutations were found in CP1, CP2 and CP3 late isolates. However, probably due to compensatory mechanisms in CP1 late isolate, only CP2 and CP3 late isolates are TA-SCV. Since thymidine is assumed to be abundant in lungs with ongoing chronic inflammation, TA-SCVs can still grow in this environment while resisting SXT treatment.

Beside thymidine auxotrophy, we observed a pantothenate auxotrophy in CP4 late isolate, which has also been previously associated with persistency in *Mycobacterium tuberculosis* [41]. The acquisition of pantothenate auxotrophy suggests that, as thymidine, pantothenate could also be

present in the lungs of CF patients. Acquisition of auxotrophies is in line with what was observed in *P. aeruginosa* CF isolates [70]. Thus, this confirms that metabolic specialization is a common phenomenon among long-term colonizers.

Other striking traits of phenotypic convergent evolution of *S. aureus* identified in this work were the increased ability to form biofilm and to persist in the intracellular niche. For CP3 and CP4 patients, the increased biofilm ability of CP3 and CP4 late isolates could be linked to a mutation in the *fakA* gene, encoding fatty acid kinase A (FakA). Indeed, several studies showed that FakA-null strains were proficient in biofilm formation [13] and deficient in the expression of virulence factors controlled by the SaeRS system [37]. Overexpression of adhesins detected in proteomic analysis could also ultimately lead to increase biofilm formation in tested clinical isolates.

Although *S. aureus* is generally not considered as an intracellular pathogen, numerous studies have demonstrated its ability to persist within host cells [15-24]. Strikingly, all the clinical isolates exhibited a greater ability to persist within CFBE-F508del epithelial cells compared to the USA300-LAC reference strain (**Fig S6**). Moreover, for the three CF patients, the *S. aureus* late isolates showed a greater ability to persist within CFBE-F508del epithelial cells compared to the early ones at day 6 post-infection. Of note, the late isolate of CP2 did not present an improved ability to persist intracellularly within CFBE-F508del epithelial cells possibly due the fact that it has adapted to a non-CF patient.

Conclusions

Our multi-omics approach allowed both confirmation of previously known mechanisms and identification of novel candidate genes and pathways involved in the persistence ability of clinical isolates. We now provide evidence that the *saeR*/*fakA* regulon and the pantothenate pathway could also be promising therapeutic targets to fight persistent *S. aureus* infections.

Our study suggests that the use of antibiotic with a good intracellular penetration should be the best therapeutic option in order to eradicate *S. aureus* from chronically infected lungs.

Acknowledgments

We thank Aurélie Hatton, Charlotte Roy and Zhicheng Zhou for their help with primary nasal epithelial cells culture.

Figure legends

Fig 1. **Selection of four pairs of *S. aureus* isolates belonging to four different STs in four patients.**

Dendrogram generated by wgsa.net from the genomes of the eight clinical isolates retrieved from the respiratory samples of four patients with chronic lung infection and four reference genomes from public databases. Branch length is proportional to the number of variant nucleotide sites within the core genes. For each patient (CP1 to CP4), the isolate taken first is called “early” while the isolate taken later is named “late”. The dates of sampling and the sequence type (ST) of the isolates are indicated. “TA” and “PA” mean that the isolate is auxotrophic for thymidine or pantothenate respectively. The name of the isolate is indicated in red when it is resistant to methicillin (MRSA). Reference strains included are PFESA1902 (ERR554197), st1307 (ERR158691), PFESA1195 (ERR554722).

Fig 2. Proteogenomic and metabolomic analysis of the four pairs of *S. aureus* isolates. (**A**) Vertical histograms show the functional classification of proteins encoded by genes with nonsynonymous mutations in the genomes of late isolates of *S. aureus* compared to early isolates. The variants were detected and annotated by the Snippy tool. Horizontal histograms show the functional classification of differentially expressed annotated proteins in late compared to early isolates of each patient. For each category, histograms represent the number of down- and up-regulated proteins from proteomic analysis using the threshold of <2 and >2, respectively. Functional classification was performed using eggNOG functional categories, followed by manual curation. Only genes and proteins with functional annotation are included. The “cellular processes and signaling” category encompasses regulatory proteins and proteins involved in cell wall and capsule synthesis. The “information storage and processing” category encompasses proteins involved in replication, translation and repair processes. The “metabolism” category encompasses proteins involved in metabolism and transport. The “virulence” category encompasses exotoxins, proteins involved in adhesion, biofilm formation and immunomodulation. (**B**) Categorization in 8 categories of altered amount of metabolites in late compared to early isolates. Metabolites were detected by carrying out 2 independent experiments performed in triplicate. TCA, Tricarboxylic acid cycle; PPP, Pentose phosphate pathway; Nucl, Nucleotides; CoA, Coenzyme A; AA, Amino acids.

Fig 3. CP4 patient highlights *S. aureus* within-host evolution. Heatmap visualization and hierarchical clustering analysis of protein (**A**) and metabolite (**B**) profiles of early/late CP4 *S. aureus* isolates. The isolates were cultured to the stationary phase in medium mimicking the respiratory fluid of cystic fibrosis patients (Cystic Fibrosis Sputum Medium or CFSM) with the addition of thymidine. **(A)** Heatmap visualization of the proteomic profiling. One experiment with three biological replicates was performed. Rows: proteins; columns: samples; color key indicates protein relative concentration value (yellow: lowest; blue: highest). List of proteins is in **S7 Table**. **(B)** Heatmap visualization of the metabolite profiling. The top 50 most changing compounds are presented. Two independent experiments with three biological replicates were performed. Rows: metabolites; columns: samples; color key indicates metabolite relative concentration value (blue: lowest; red: highest). List of metabolites is in **S8 Table**.

Fig 4. Growth of late *S. aureus* clinical isolates in CFSM. Growth curves were carried out in CFSM, with or without the addition of thymidine or pantothenate. The results shown correspond to a representative experiment for CP1_late isolate (**A**), CP2_late and CP3_late isolates (**B**) and CP4_late isolate (**C**). The orange and green curves correspond to bacterial growth in media supplemented with either thymidine or pantothenate; the red and blue curves, to bacterial growth in medium without thymidine or pantothenate. WT, USA300-LAC.

Fig 5. Quantification of biofilm formation of *S. aureus* clinical isolates. Biofilm formation quantification was performed using the crystal violet microtiter assay in BHI medium with 1% glucose. Results shown are the mean ±SD for three independent experiments performed in triplicate. Statistical significance was measured using a two-tail Student's t-test when biofilm production of a late isolate was compared with biofilm production of cognate early isolate from the same patient. ** indicates p-value of <0.001 whereas ns indicates p-values>0.05.

Fig 6. Intracellular persistence of *S. aureus* clinical isolates in CFBE-F508del epithelial cell line. Bronchial CFBE epithelial cell line (CFBE-F508del homozygous for the F508del-CFTR mutation) was infected with the control strain USA300-LAC and clinical isolates. Gentamicin was present throughout the experiment to prevent extracellular bacterial growth and new infection. Bacterial load inside cells were evaluated by CFU enumeration at 6 days after infection. Results are normalized with USA300-LAC strain as a reference and expressed as a fold change of CFUs. Results shown are the mean ±SD for two independent experiments performed in triplicate (results at 3 days post infection and within

CFBE_WT are shown in **Fig S6**). Statistical analysis was performed by unpaired two-tailed Student's t test.

Fig 7. Intracellular persistence of CP4 *S. aureus* clinical isolates within primary F508del epithelial own patient cells.

Primary nasal epithelial cells retrieved from a healthy donor (WT primary cells) and from the CP4 patient (CP4 primary cells with F508del +/+ CFTR mutation) were infected with the control strain USA300-LAC and CP4 isolates. Gentamicin was present throughout the experiment to prevent extracellular bacterial growth and new infection. Bacterial loads inside cells were evaluated by CFU enumeration at 3 and 6 days after infection. Results are normalized with USA300-LAC (WT) strain as a reference and expressed as a fold change of CFUs. Results shown are the mean ±SD for one experiment performed in triplicate.

References

1. Sethi S, Murphy TF. Infection in the pathogenesis and course of chronic obstructive pulmonary disease. The New England journal of medicine. 2008;359(22):2355-65. doi: 10.1056/NEJMra0800353.

2. Stoltz DA, Meyerholz DK, Welsh MJ. Origins of cystic fibrosis lung disease. The New England journal of medicine. 2015;372(16):1574-5. doi: 10.1056/NEJMc1502191.

3. Jesenak M, Banovcin P, Jesenakova B, Babusikova E. Pulmonary manifestations of primary immunodeficiency disorders in children. Frontiers in pediatrics. 2014;2:77. doi: 10.3389/fped.2014.00077.

4. Wijers CD, Chmiel JF, Gaston BM. Bacterial infections in patients with primary ciliary dyskinesia: Comparison with cystic fibrosis. Chronic respiratory disease. 2017;14(4):392-406. doi: 10.1177/1479972317694621.

5. Goerke C, Wolz C. Adaptation of Staphylococcus aureus to the cystic fibrosis lung. International journal of medical microbiology : IJMM. 2010;300(8):520-5. doi: 10.1016/j.ijmm.2010.08.003.

6. Didelot X, Walker AS, Peto TE, Crook DW, Wilson DJ. Within-host evolution of bacterial pathogens. Nature reviews Microbiology. 2016;14(3):150-62. doi: 10.1038/nrmicro.2015.13.

7. Marvig RL, Sommer LM, Molin S, Johansen HK. Convergent evolution and adaptation of Pseudomonas aeruginosa within patients with cystic fibrosis. Nature genetics. 2015;47(1):57-64. doi: 10.1038/ng.3148.

8. Diaz Caballero J, Clark ST, Coburn B, Zhang Y, Wang PW, Donaldson SL, et al. Selective Sweeps and Parallel Pathoadaptation Drive Pseudomonas aeruginosa Evolution in the Cystic Fibrosis Lung. mBio. 2015;6(5):e00981-15. doi: 10.1128/mBio.00981-15.

9. Haussler S, Tummler B, Weissbrodt H, Rohde M, Steinmetz I. Small-colony variants of Pseudomonas aeruginosa in cystic fibrosis. Clinical infectious diseases : an official publication of the Infectious Diseases Society of America. 1999;29(3):621-5.

10. McAdam PR, Holmes A, Templeton KE, Fitzgerald JR. Adaptive evolution of Staphylococcus aureus during chronic endobronchial infection of a cystic fibrosis patient. PloS one. 2011;6(9):e24301. doi: 10.1371/journal.pone.0024301.

11. Lopez-Collazo E, Jurado T, de Dios Caballero J, Perez-Vazquez M, Vindel A, Hernandez-Jimenez E, et al. In vivo attenuation and genetic evolution of a ST247-SCCmecI MRSA clone after 13 years of pathogenic bronchopulmonary colonization in a patient with cystic fibrosis: implications of the innate immune response. Mucosal immunology. 2015;8(2):362-71. doi: 10.1038/mi.2014.73.

12. Zapotoczna M, O'Neill E, O'Gara JP. Untangling the Diverse and Redundant Mechanisms of Staphylococcus aureus Biofilm Formation. PLoS pathogens. 2016;12(7):e1005671. doi: 10.1371/journal.ppat.1005671.

13. Sabirova JS, Hernalsteens JP, De Backer S, Xavier BB, Moons P, Turlej-Rogacka A, et al. Fatty acid kinase A is an important determinant of biofilm formation in Staphylococcus aureus USA300. BMC genomics. 2015;16:861. doi: 10.1186/s12864-015-1956-8.

14. Schwartbeck B, Birtel J, Treffon J, Langhanki L, Mellmann A, Kale D, et al. Dynamic in vivo mutations within the ica operon during persistence of Staphylococcus aureus in the airways of cystic fibrosis patients. PLoS pathogens. 2016;12(11):e1006024. doi: 10.1371/journal.ppat.1006024.

15. Garzoni C, Francois P, Huyghe A, Couzinet S, Tapparel C, Charbonnier Y, et al. A global view of Staphylococcus aureus whole genome expression upon internalization in human epithelial cells. BMC genomics. 2007;8:171. doi: 10.1186/1471-2164-8-171.

16. Garzoni C, Kelley WL. Staphylococcus aureus: new evidence for intracellular persistence. Trends in microbiology. 2009;17(2):59-65. doi: 10.1016/j.tim.2008.11.005.

17. Kalinka J, Hachmeister M, Geraci J, Sordelli D, Hansen U, Niemann S, et al. Staphylococcus aureus isolates from chronic osteomyelitis are characterized by high host cell invasion and intracellular adaptation, but still induce inflammation. International journal of medical microbiology : IJMM. 2014;304(8):1038-49. doi: 10.1016/j.ijmm.2014.07.013.

18. Mitchell G, Grondin G, Bilodeau G, Cantin AM, Malouin F. Infection of polarized airway epithelial cells by normal and small-colony variant strains of Staphylococcus aureus is increased in cells with abnormal cystic fibrosis transmembrane conductance regulator function and is influenced by NF-kappaB. Infection and immunity. 2011;79(9):3541-51. doi: 10.1128/IAI.00078-11.

19. Proctor RA, von Eiff C, Kahl BC, Becker K, McNamara P, Herrmann M, et al. Small colony variants: a pathogenic form of bacteria that facilitates persistent and recurrent infections. Nature reviews Microbiology. 2006;4(4):295-305. doi: 10.1038/nrmicro1384.

20. Rollin G, Tan X, Tros F, Dupuis M, Nassif X, Charbit A, et al. Intracellular Survival of Staphylococcus aureus in Endothelial Cells: A Matter of Growth or Persistence. Frontiers in microbiology. 2017;8:1354. doi: 10.3389/fmicb.2017.01354.

21. Sendi P, Proctor RA. Staphylococcus aureus as an intracellular pathogen: the role of small colony variants. Trends in microbiology. 2009;17(2):54-8. doi: 10.1016/j.tim.2008.11.004.

22. Tuchscherr L, Heitmann V, Hussain M, Viemann D, Roth J, von Eiff C, et al. Staphylococcus aureus small-colony variants are adapted phenotypes for intracellular persistence. The Journal of infectious diseases. 2010;202(7):1031-40. doi: 10.1086/656047.

23. Tuchscherr L, Medina E, Hussain M, Volker W, Heitmann V, Niemann S, et al. Staphylococcus aureus phenotype switching: an effective bacterial strategy to escape host immune response and establish a chronic infection. EMBO molecular medicine. 2011;3(3):129-41. doi: 10.1002/emmm.201000115.

24. von Eiff C, Becker K, Metze D, Lubritz G, Hockmann J, Schwarz T, et al. Intracellular persistence of Staphylococcus aureus small-colony variants within keratinocytes: a cause for antibiotic treatment failure in a patient with darier's disease. Clinical infectious diseases : an official publication of the Infectious Diseases Society of America. 2001;32(11):1643-7. doi: 10.1086/320519.

25. Branger C, Gardye C, Lambert-Zechovsky N. Persistence of Staphylococcus aureus strains among cystic fibrosis patients over extended periods of time. Journal of medical microbiology. 1996;45(4):294-301. doi: 10.1099/00222615-45-4-294.

26. Kahl BC, Duebbers A, Lubritz G, Haeberle J, Koch HG, Ritzerfeld B, et al. Population dynamics of persistent Staphylococcus aureus isolated from the airways of cystic fibrosis patients during a 6-year prospective study. Journal of clinical microbiology. 2003;41(9):4424-7. doi: 10.1128/JCM.41.9.4424-4427.2003.

27. Kriegeskorte A, Grubmuller S, Huber C, Kahl BC, von Eiff C, Proctor RA, et al. Staphylococcus aureus small colony variants show common metabolic features in central metabolism irrespective of the underlying auxotrophism. Frontiers in cellular and infection microbiology. 2014;4:141. doi: 10.3389/fcimb.2014.00141.

28. Garcia-Betancur JC, Goni-Moreno A, Horger T, Schott M, Sharan M, Eikmeier J, et al. Cell differentiation defines acute and chronic infection cell types in Staphylococcus aureus. eLife. 2017;6. doi: 10.7554/eLife.28023.

29. Tuchscherr L, Kreis CA, Hoerr V, Flint L, Hachmeister M, Geraci J, et al. Staphylococcus aureus develops increased resistance to antibiotics by forming dynamic small colony variants during chronic osteomyelitis. The Journal of antimicrobial chemotherapy. 2016;71(2):438-48. doi: 10.1093/jac/dkv371.

30. Sadowska B, Bonar A, von Eiff C, Proctor RA, Chmiela M, Rudnicka W, et al. Characteristics of Staphylococcus aureus, isolated from airways of cystic fibrosis patients, and their small colony variants. FEMS immunology and medical microbiology. 2002;32(3):191-7.

31. Das S, Lindemann C, Young BC, Muller J, Osterreich B, Ternette N, et al. Natural mutations in a Staphylococcus aureus virulence regulator attenuate cytotoxicity but permit bacteremia and abscess formation. Proceedings of the National Academy of Sciences of the United States of America. 2016;113(22):E3101-10. doi: 10.1073/pnas.1520255113.

32. Suligoy CM, Lattar SM, Noto Llana M, Gonzalez CD, Alvarez LP, Robinson DA, et al. Mutation of Agr Is Associated with the Adaptation of Staphylococcus aureus to the Host during Chronic Osteomyelitis. Frontiers in cellular and infection microbiology. 2018;8:18. doi: 10.3389/fcimb.2018.00018.

33. Tuchscherr L, Loffler B. Staphylococcus aureus dynamically adapts global regulators and virulence factor expression in the course from acute to chronic infection. Current genetics. 2016;62(1):15-7. doi: 10.1007/s00294-015-0503-0.

34. Viberg LT, Sarovich DS, Kidd TJ, Geake JB, Bell SC, Currie BJ, et al. Within-Host Evolution of Burkholderia pseudomallei during Chronic Infection of Seven Australasian Cystic Fibrosis Patients. mBio. 2017;8(2). doi: 10.1128/mBio.00356-17.

35. Lee AH, Flibotte S, Sinha S, Paiero A, Ehrlich RL, Balashov S, et al. Phenotypic diversity and genotypic flexibility of Burkholderia cenocepacia during long-term chronic infection of cystic fibrosis lungs. Genome research. 2017;27(4):650-62. doi: 10.1101/gr.213363.116.

36. Garofalo A, Giai C, Lattar S, Gardella N, Mollerach M, Kahl BC, et al. The length of the Staphylococcus aureus protein A polymorphic region regulates inflammation: impact on acute and chronic infection. The Journal of infectious diseases. 2012;206(1):81-90. doi: 10.1093/infdis/jis311.

37. Ericson ME, Subramanian C, Frank MW, Rock CO. Role of Fatty Acid Kinase in Cellular Lipid Homeostasis and SaeRS-Dependent Virulence Factor Expression in Staphylococcus aureus. mBio. 2017;8(4). doi: 10.1128/mBio.00988-17.

38. Askarian F, Uchiyama S, Valderrama JA, Ajayi C, Sollid JU, van Sorge NM, et al. Serine-Aspartate Repeat Protein D Increases Staphylococcus aureus Virulence and Survival in Blood. Infection and immunity. 2017;85(1). doi: 10.1128/IAI.00559-16.

39. Connolly J, Boldock E, Prince LR, Renshaw SA, Whyte MK, Foster SJ. Identification of Staphylococcus aureus Factors Required for Pathogenicity and Growth in Human Blood. Infection and immunity. 2017;85(11). doi: 10.1128/IAI.00337-17.

40. Kriegeskorte A, Block D, Drescher M, Windmuller N, Mellmann A, Baum C, et al. Inactivation of thyA in Staphylococcus aureus attenuates virulence and has a strong impact on metabolism and virulence gene expression. mBio. 2014;5(4):e01447-14. doi: 10.1128/mBio.01447-14.

41. Sambandamurthy VK, Wang X, Chen B, Russell RG, Derrick S, Collins FM, et al. A pantothenate auxotroph of Mycobacterium tuberculosis is highly attenuated and protects mice against tuberculosis. Nature medicine. 2002;8(10):1171-4. doi: 10.1038/nm765.

42. Oogai Y, Yamaguchi M, Kawada-Matsuo M, Sumitomo T, Kawabata S, Komatsuzawa H. Lysine and Threonine Biosynthesis from Aspartate Contributes to Staphylococcus aureus Growth in Calf Serum. Applied and environmental microbiology. 2016;82(20):6150-7. doi: 10.1128/AEM.01399-16.

814 43. Spry C, Kirk K, Saliba KJ. Coenzyme A biosynthesis: an antimicrobial drug target.
815 FEMS microbiology reviews. 2008;32(1):56-106. doi: 10.1111/j.1574-6976.2007.00093.x.

816 44. Chatterjee I, Kriegeskorte A, Fischer A, Deiwick S, Theimann N, Proctor RA, et al. In
817 vivo mutations of thymidylate synthase (encoded by thyA) are responsible for thymidine dependency
818 in clinical small-colony variants of Staphylococcus aureus. Journal of bacteriology. 2008;190(3):834-
819 42. doi: 10.1128/JB.00912-07.

820 45. Palmer KL, Aye LM, Whiteley M. Nutritional cues control Pseudomonas aeruginosa
821 multicellular behavior in cystic fibrosis sputum. Journal of bacteriology. 2007;189(22):8079-87. doi:
822 10.1128/JB.01138-07.

823 46. Argudin MA, Roisin S, Dodemont M, Nonhoff C, Deplano A, Denis O. Mutations at the
824 Ribosomal S10 Gene in Clinical Strains of Staphylococcus aureus with Reduced Susceptibility to
825 Tigecycline. Antimicrobial agents and chemotherapy. 2018;62(1). doi: 10.1128/AAC.01852-17.

826 47. Bolger AM, Lohse M, Usadel B. Trimmomatic: a flexible trimmer for Illumina sequence
827 data. Bioinformatics. 2014;30(15):2114-20. doi: 10.1093/bioinformatics/btu170.

828 48. Bankevich A, Nurk S, Antipov D, Gurevich AA, Dvorkin M, Kulikov AS, et al. SPAdes:
829 a new genome assembly algorithm and its applications to single-cell sequencing. Journal of
830 computational biology : a journal of computational molecular cell biology. 2012;19(5):455-77. doi:
831 10.1089/cmb.2012.0021.

832 49. Seemann T. Prokka: rapid prokaryotic genome annotation. Bioinformatics.
833 2014;30(14):2068-9. doi: 10.1093/bioinformatics/btu153.

834 50. Overbeek R, Olson R, Pusch GD, Olsen GJ, Davis JJ, Disz T, et al. The SEED and
835 the Rapid Annotation of microbial genomes using Subsystems Technology (RAST). Nucleic acids
836 research. 2014;42(Database issue):D206-14. doi: 10.1093/nar/gkt1226.

837 51. Ehrhardt C, Collnot EM, Baldes C, Becker U, Laue M, Kim KJ, et al. Towards an in
838 vitro model of cystic fibrosis small airway epithelium: characterisation of the human bronchial epithelial
839 cell line CFBE41o. Cell and tissue research. 2006;323(3):405-15. doi: 10.1007/s00441-005-0062-7.

840 52. Pranke IM, Hatton A, Simonin J, Jais JP, Le Pimpec-Barthes F, Carsin A, et al.
841 Correction of CFTR function in nasal epithelial cells from cystic fibrosis patients predicts improvement
842 of respiratory function by CFTR modulators. Scientific reports. 2017;7(1):7375. doi: 10.1038/s41598-
843 017-07504-1.

844 53. Wisniewski JR, Zougman A, Mann M. Combination of FASP and StageTip-based
845 fractionation allows in-depth analysis of the hippocampal membrane proteome. Journal of proteome
846 research. 2009;8(12):5674-8. doi: 10.1021/pr900748n.

847 54. Lipecka J, Chhuon C, Bourderioux M, Bessard MA, van Endert P, Edelman A, et al.
848 Sensitivity of mass spectrometry analysis depends on the shape of the filtration unit used for filter
849 aided sample preparation (FASP). Proteomics. 2016;16(13):1852-7. doi: 10.1002/pmic.201600103.

850 55. Vallenet D, Labarre L, Rouy Z, Barbe V, Bocs S, Cruveiller S, et al. MaGe: a microbial
851 genome annotation system supported by synteny results. Nucleic acids research. 2006;34(1):53-65.
852 doi: 10.1093/nar/gkj406.

853 56. Fu L, Niu B, Zhu Z, Wu S, Li W. CD-HIT: accelerated for clustering the next-
854 generation sequencing data. Bioinformatics. 2012;28(23):3150-2. doi: 10.1093/bioinformatics/bts565.

855 57. Cox J, Mann M. MaxQuant enables high peptide identification rates, individualized
856 p.p.b.-range mass accuracies and proteome-wide protein quantification. Nature biotechnology.
857 2008;26(12):1367-72. doi: 10.1038/nbt.1511.

858 58. Tyanova S, Temu T, Sinitcyn P, Carlson A, Hein MY, Geiger T, et al. The Perseus
859 computational platform for comprehensive analysis of (prote)omics data. Nature methods.
860 2016;13(9):731-40. doi: 10.1038/nmeth.3901.

861 59. Huerta-Cepas J, Forslund K, Coelho LP, Szklarczyk D, Jensen LJ, von Mering C, et
862 al. Fast Genome-Wide Functional Annotation through Orthology Assignment by eggNOG-Mapper.
863 Molecular biology and evolution. 2017;34(8):2115-22. doi: 10.1093/molbev/msx148.

60. Fuchs S, Mehlan H, Bernhardt J, Hennig A, Michalik S, Surmann K, et al. AureoWiki The repository of the Staphylococcus aureus research and annotation community. International journal of medical microbiology : IJMM. 2017. doi: 10.1016/j.ijmm.2017.11.011.

61. Mackay GM, Zheng L, van den Broek NJ, Gottlieb E. Analysis of Cell Metabolism Using LC-MS and Isotope Tracers. Methods in enzymology. 2015;561:171-96. doi: 10.1016/bs.mie.2015.05.016.

62. Xia J, Wishart DS. Using MetaboAnalyst 3.0 for Comprehensive Metabolomics Data Analysis. Current protocols in bioinformatics. 2016;55:14 0 1- 0 91. doi: 10.1002/cpbi.11.

63. Painter KL, Krishna A, Wigneshweraraj S, Edwards AM. What role does the quorum-sensing accessory gene regulator system play during Staphylococcus aureus bacteremia? Trends in microbiology. 2014;22(12):676-85. doi: 10.1016/j.tim.2014.09.002.

64. Shopsin B, Eaton C, Wasserman GA, Mathema B, Adhikari RP, Agolory S, et al. Mutations in agr do not persist in natural populations of methicillin-resistant Staphylococcus aureus. The Journal of infectious diseases. 2010;202(10):1593-9. doi: 10.1086/656915.

65. Liu Q, Yeo WS, Bae T. The SaeRS Two-Component System of Staphylococcus aureus. Genes. 2016;7(10). doi: 10.3390/genes7100081.

66. Montgomery CP, Boyle-Vavra S, Daum RS. Importance of the global regulators Agr and SaeRS in the pathogenesis of CA-MRSA USA300 infection. PloS one. 2010;5(12):e15177. doi: 10.1371/journal.pone.0015177.

67. Cassat JE, Hammer ND, Campbell JP, Benson MA, Perrien DS, Mrak LN, et al. A secreted bacterial protease tailors the Staphylococcus aureus virulence repertoire to modulate bone remodeling during osteomyelitis. Cell host & microbe. 2013;13(6):759-72. doi: 10.1016/j.chom.2013.05.003.

68. Askarian F, Ajayi C, Hanssen AM, van Sorge NM, Pettersen I, Diep DB, et al. The interaction between Staphylococcus aureus SdrD and desmoglein 1 is important for adhesion to host cells. Scientific reports. 2016;6:22134. doi: 10.1038/srep22134.

69. Kriegeskorte A, Lore NI, Bragonzi A, Riva C, Kelkenberg M, Becker K, et al. Thymidine-Dependent Staphylococcus aureus Small-Colony Variants Are Induced by Trimethoprim-Sulfamethoxazole (SXT) and Have Increased Fitness during SXT Challenge. Antimicrobial agents and chemotherapy. 2015;59(12):7265-72. doi: 10.1128/AAC.00742-15.

70. La Rosa R, Johansen HK, Molin S. Convergent Metabolic Specialization through Distinct Evolutionary Paths in Pseudomonas aeruginosa. mBio. 2018;9(2). doi: 10.1128/mBio.00269-18.

Additional files

Table S1: Basic assembly metrics. (.doc)

Table S2: List of genes missing in late isolates compared to early isolates. (.xls)

Table S3: List of nonsynonymous mutations present in late isolates compared to early isolates. (.xls)

Table S4: Stop codons in CP clones compared to reference strains. (.doc)

Table S5: Nonsynonymous mutations in clones of at least 3 of the 4 CP patients. (.doc)

Table S6: Convergent evolution in late isolates. (.doc)

Table S7: List of proteins with a detection difference of at least 2 in log2(intensity) after normalization in late isolates compared to early isolates. (.xls)

Table S8: List of metabolites with altered amount in the late isolates compared to early isolates. (.xls)

Figure S1: Heatmaps showing comparison of protein and metabolite profiles of early/late *S. aureus* isolates.

Figure S2: Colony morphology of CP2_late and CP3_late isolates. Bacteria were grown on BHI agar incubated 12h at 37°C.

Figure S3: Growth curves of early *S. aureus* clinical isolates in CFSM.

Figure S4: Quantification of biofilm formation of *S. aureus* clinical isolates.

Figure S5: Intracellular growth curves of reference *S. aureus* isolates in CFBE epithelial cell line.

Figure S6: Intracellular persistence of *S. aureus* clinical isolates in CFBE-F508del epithelial cell line. (.pdf)

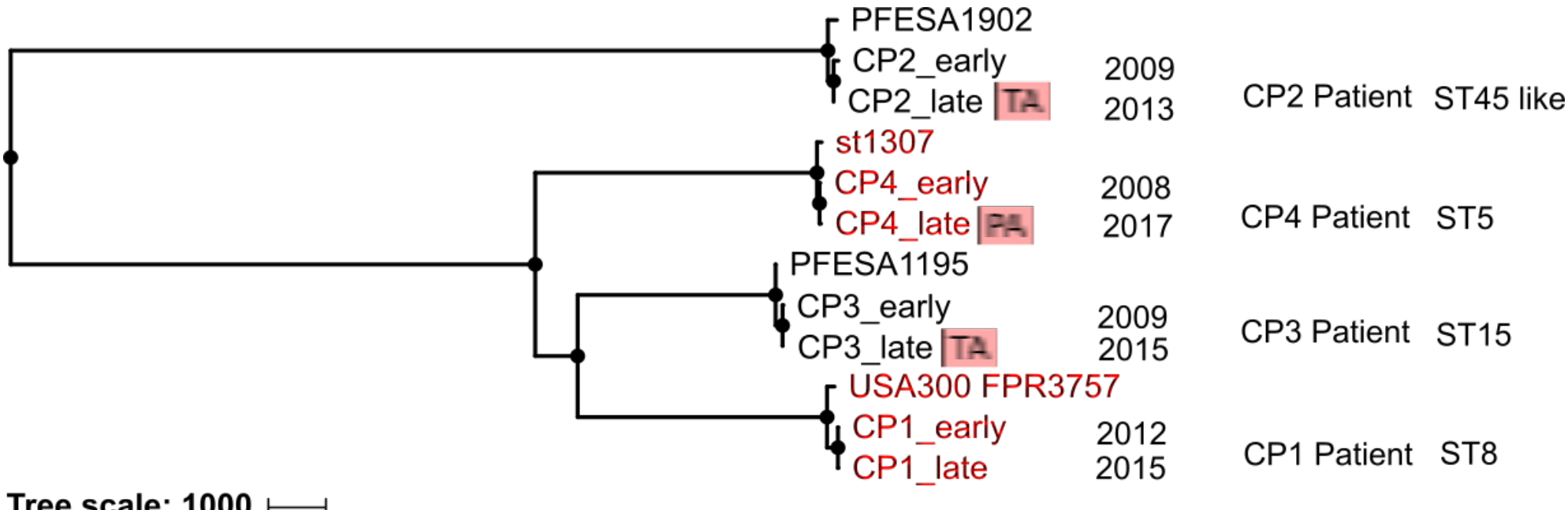
PFESA1902
CP2_early
CP2_late
2009
2013
CP2 Patient
ST45 like
st1307
CP4_early
CP4_late
2008
2017
CP4 Patient
ST5
PFESA1195
CP3_early
CP3_late
2009
2015
CP3 Patient
ST15
USA300 FPR3757
CP1_early
CP1_late
2012
2015
CP1 Patient
ST8
Tree scale: 1000

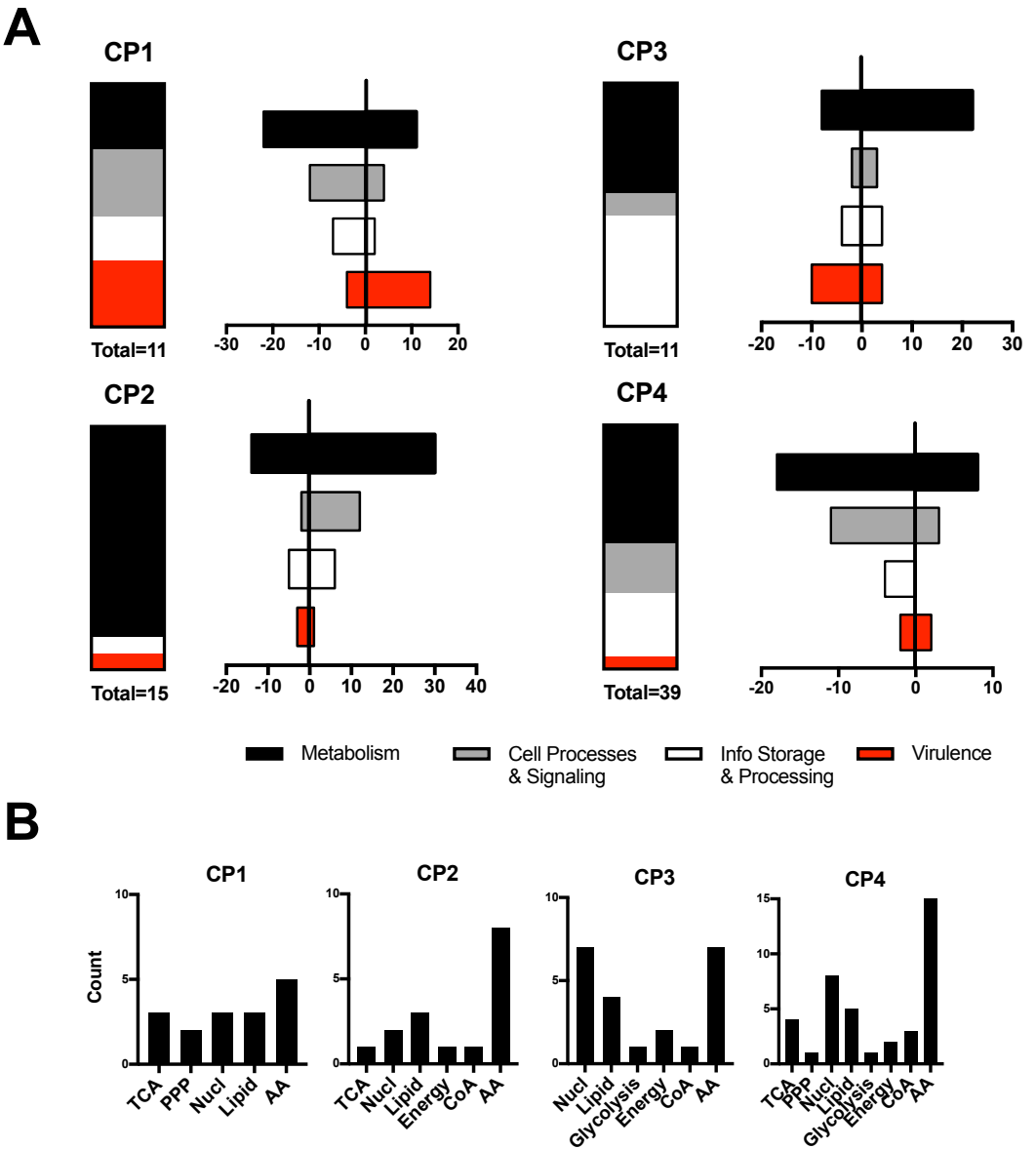
A
CP1
Total=11
-30 -20 -10 0 10 20
CP3
Total=11
-20 -10 0 10 20 30
CP2
Total=15
-20 -10 0 10 20 30 40
CP4
Total=39
-20 -10 0 10
Metabolism
Cell Processes & Signaling
Info Storage & Processing
Virulence
B
CP1
CP2
CP3
CP4
Count
0 5 10
TCA PPP Nucl Lipid AA
TCA Nucl Lipid Energy CoA AA
Nucl Lipid Glycolysis Energy CoA AA
0 5 10 15
TCA PPP Nucl Lipid Glycolysis Energy CoA AA

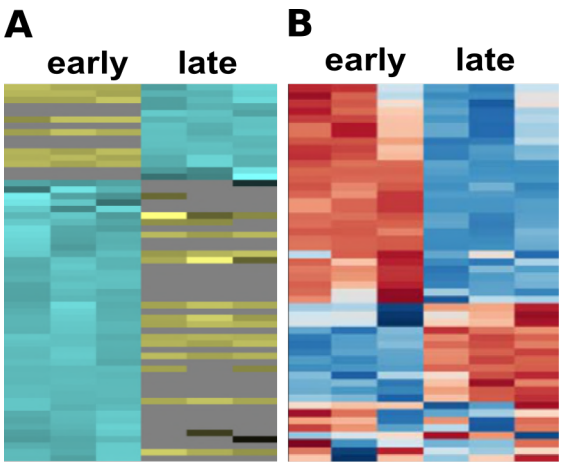

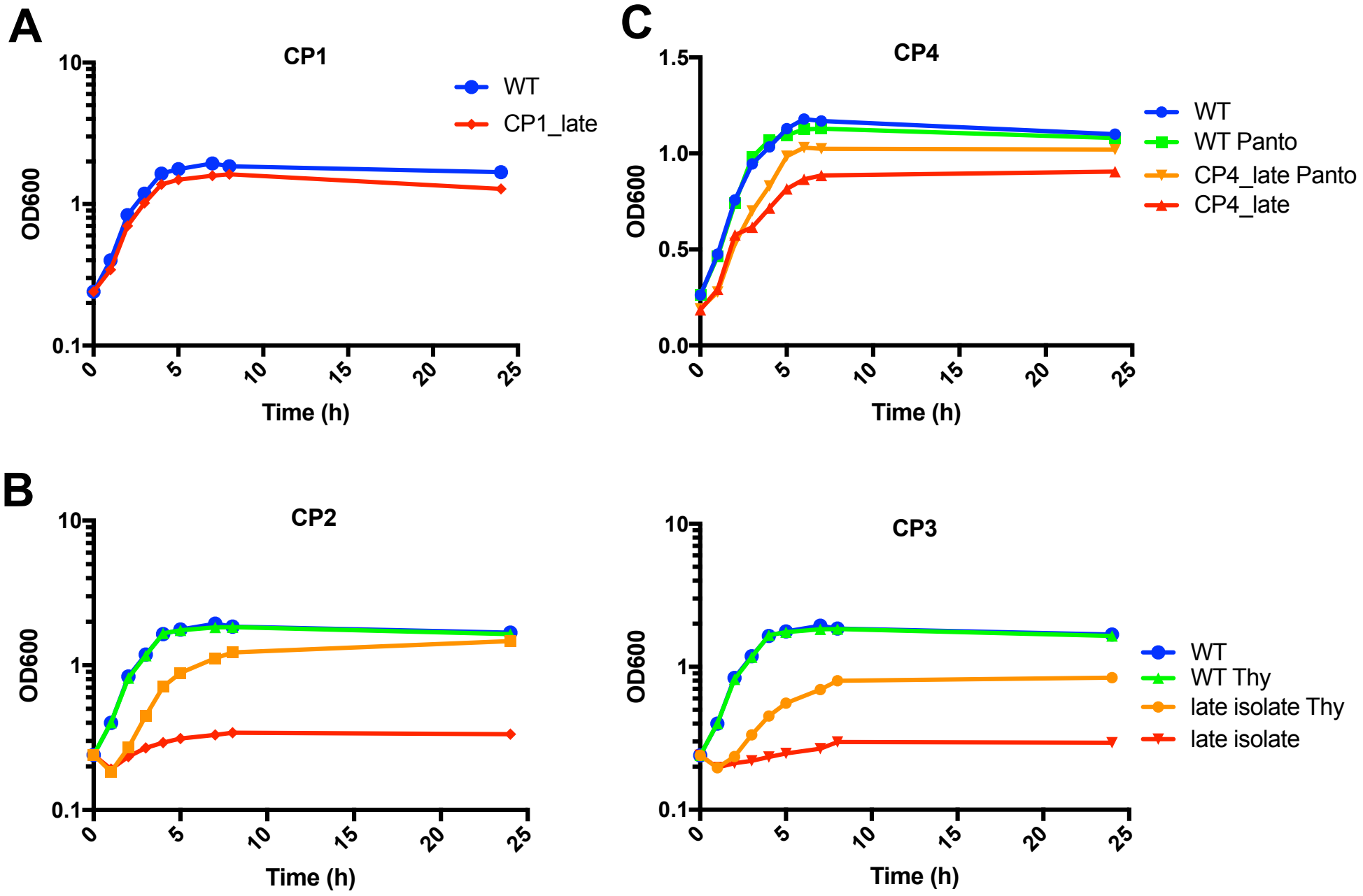
A
CP1
WT
CP1_late
OD600
Time (h)
B
CP2
C
CP4
WT
WT Panto
CP4_late Panto
CP4_late
CP3
WT
WT Thy
late isolate Thy
late isolate

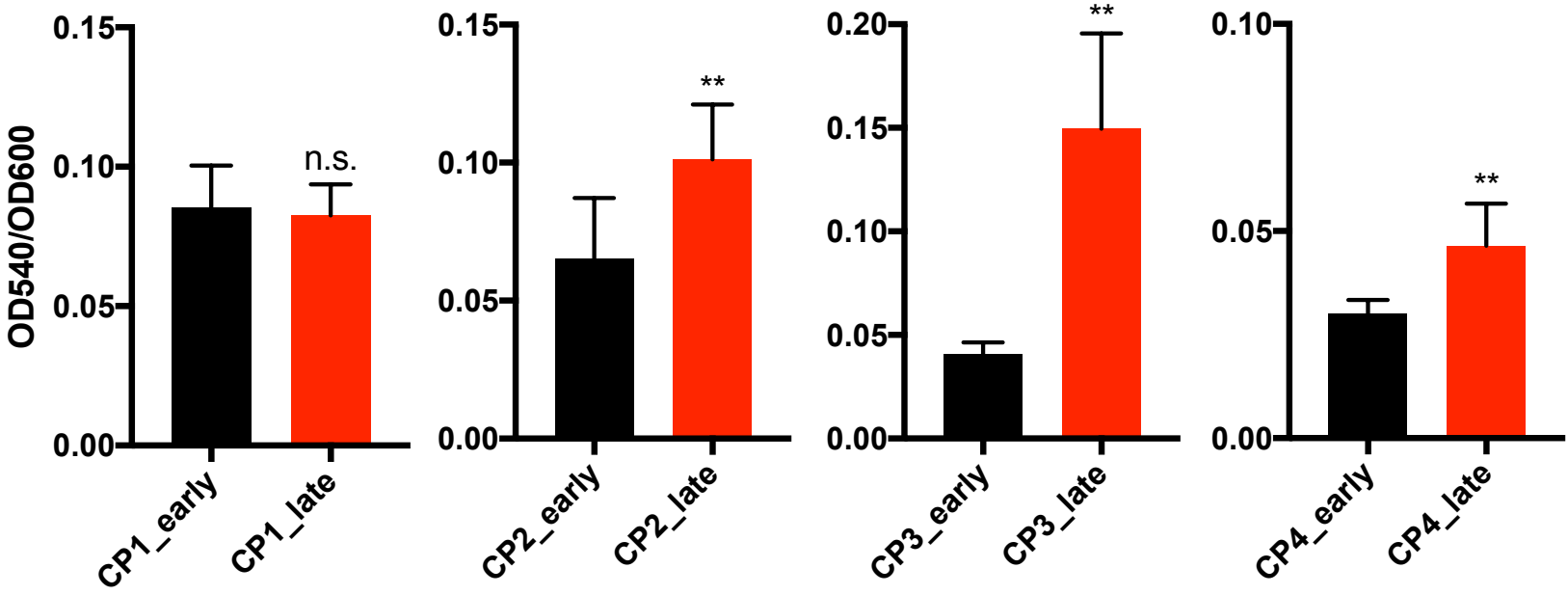
OD540/OD600
0.15
0.10
0.05
0.00
n.s.
CP1_early
CP1_late
0.15
0.10
0.05
0.00
**
CP2_early
CP2_late
0.20
0.15
0.10
0.05
0.00
**
CP3_early
CP3_late
0.10
0.05
0.00
**
CP4_early
CP4_late

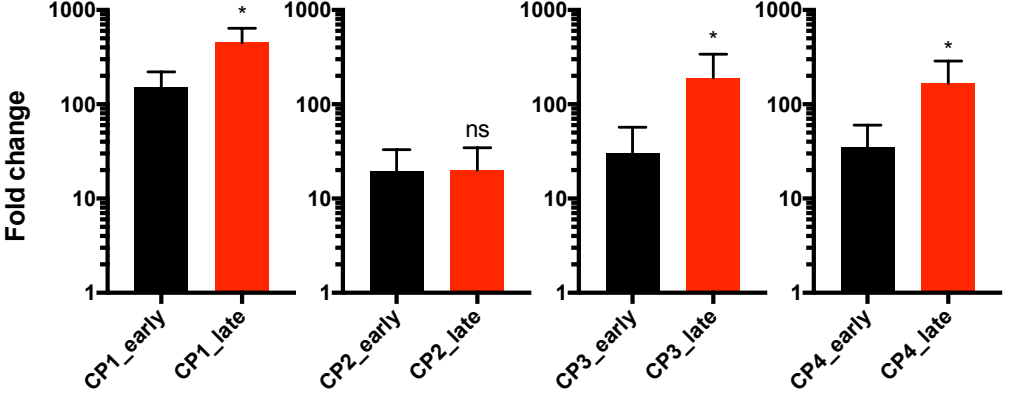
Fold change
1000
100
10
1
*
ns
*
*
CP1_early
CP1_late
CP2_early
CP2_late
CP3_early
CP3_late
CP4_early
CP4_late

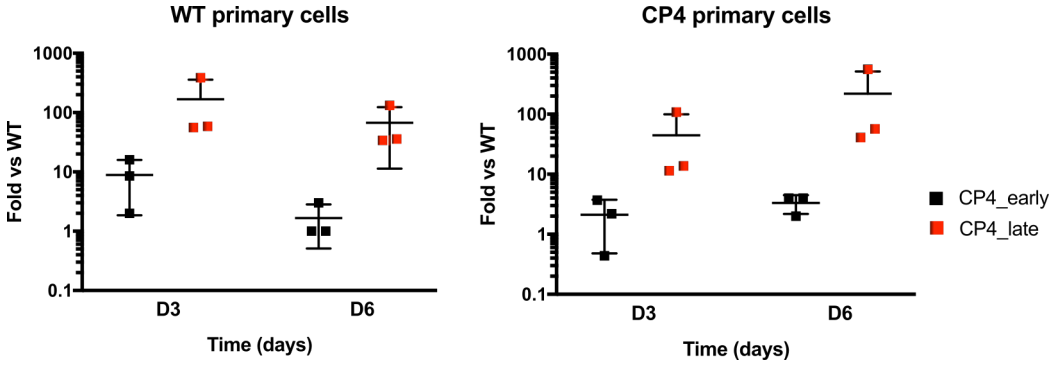
WT primary cells
CP4 primary cells
Fold vs WT
1000
100
10
1
0.1
D3
D6
Time (days)
CP4_early
CP4_late